2019

Computational Characterization of the Cellular Origins of Electroencephalography

Shane Hesprich

Scott A. Beardsley

2019 9th International IEEE/EMBS Conference on Neural Engineering (NER), (March 20-23, 2019): 352-355. DOI.

Computational Characterization of the Cellular Origins of Electroencephalography*

Shane Hesprich
Department Biomedical Engineering, Marquette University, Milwaukee, WI
Scott Beardsley
Department of Biomedical Engineering, Marquette University and Medical College of Wisconsin, Milwaukee, WI

Abstract:

Despite the widespread use of Electroecephalography (EEG) as an imaging modality, neural generators of current dipoles measured by EEG at the scalp are not fully understood. Here, we use two morphologically accurate multicompartments neuron models (layer IV pyramidal cell and layer V spiny stellate cell) to characterize how spiking neurons generate current dipoles in response to synaptic input. The simulations indicate that the dipole generated by synaptic inputs required to drive a pyramidal cell to threshold is smaller

than the dipole associated the action potential itself. These results suggest a greater role of spiking neural activity toward EEG signals measured at the scalp than typically assumed.

SECTION I. Introduction

Electroencephalography (EEG) is a commonly used technique to measure electrical activity of the brain. It is used clinically to diagnose conditions from Alzheimer's to Epilepsy. EEG has also permeated almost every area of neuroscience research, from mechanistic studies of motor control or sensory perception to neurological dysfunction.

Though the mathematical principles by which electromagnetic fields propagate from the cortical surface to the scalp are well established [1], the link between neural generators of current dipoles that underlay EEG signals is under-explored [2]. The standard assumption is that EEG signals originate from post synaptic potentials on synchronously firing pyramidal cells. While this is a reasonable mechanism, other sources of current flow may also play a role in the generation of scalp potentials. The objective of the research reported here was to computationally investigate the components of cellular activity which most contribute to current dipoles associated with EEG. Murakami has computationally examined the dipoles generated by spiking neurons after being directly stimulated [8]. The simulations presented here expand the approach to examine individually spiking pyramidal cells and the relative contributions of post-synaptic potentials (PSPs) and spiking to the cellular current dipole following synaptic stimulation of the neuron.

SECTION II. Approach

In order to investigate how neuronal activity contributes to the current dipoles associated with EEG, we characterized layer IV pyramidal cells and spiny stellate cells under several conditions. Morphologically accurate multi-compartment neuron models were simulated to quantify the form and magnitude of the dipole response to synaptic input versus spiking activity.

A. Cell Models

Simulations of individual three dimensional neurons were conducted using the NEURON simulation environment [3]. Two neuron models were selected from the NEURON database (obtained from ModelDB accession number 2488 [4]), a model pyramidal cell and a spiny stellate cell. Details of the models including intrinsic currents and conductances used can be found in [5].

Chattering Pyramidal Cell

The model pyramidal cell is a digital reconstruction of a layer V pyramidal cell located in the visual cortex of a cat. The dynamics of the ionic currents in combination with the dendritic morphology of the original pyramidal cell model caused the cell to fire in a chattering pattern (firing multiple subsequent action potentials) in response to a stimulus impulse.

Regularly Spiking Pyramidal Cell

Not all pyramidal cells exhibit chattering behaviour [5]. In order to also explore the current dipoles created by regularly spiking pyramidal cells, the calcium and calcium dependent potassium currents, which drive the chattering behaviour, were removed from all segments of a separate pyramidal cell model to characterize the dipole contribution of single action potentials in response to a stimulus impulse.

Interneuron

The brain contains several hundred different types of neurons [6]. As a first step toward characterizing the contribution of interneurons, we used a spiny stellate cell, which is one of the most common interneurons in the

brain [7]. The spiny stellate model used was a digital reconstruction of a layer IV spiny stellate cell from the somatosensory cortex of a rat.

B. Calculation of Current Dipole Moment

The methodology for calculating the current dipoles resulting from stimulation of the NEURON cell models is a modified version of the approach used by Murakami and colleagues [8]. For each simulation, the current dipole was estimated using one of the three dimensional NEURON models discussed above. Each compartment of the neuron model was considered to have its own current dipole $\vec{Q}_k$, denoting the vector quantity of the current dipole $\vec{Q}$ oriented along the x, y, and z, axes, for the k_{th} compartment. $\vec{Q}_k$ was calculated as:

$$\vec{Q}_k = IL_k d\vec{r} \quad (1)$$

where I_k is the longitudinal current in the compartment, L_k, is the length of the compartment and $d\vec{r}$ is the compartment's unit direction vector; defined as distance from the compartment's most proximal xyz coordinates to the most distal xyz coordinates divided by the vector's magnitude. The longitudinal current, *I*, was given by:

$$I_k = \frac{-\pi * a_k^2}{\rho_L} \frac{\partial v}{\partial x} \quad (2)$$

where a_k is the radius of the compartment, ρ_L is the longitudinal resistivity, and $\frac{\partial v}{\partial x}$ is the partial derivative of voltage with respect to length along the compartment. The current dipole of the entire cell was calculated by taking a vector sum of dipoles across all compartments. Finally, since EEG electrodes are located on the scalp, only dipole contributions perpendicular to the pial surface were considered, by taking the dot product between the cellular current dipole vector, $\vec{Q}$, and the unit vector perpendicular to the pial surface, $d\vec{r}$. For pyramidal cells the unit vector perpendicular to the pial surface was defined as to be parallel to the primary apical dendrite. Since spiny stellate cells do not have a documented orientation with respect to the pial surface, a $d\vec{r}$ was selected which maximized the dipole generated. Using this approach the complex geometry and electrophysiology of each neuron model was reduced to a single time series referred to as a Dipole Response Function (DRF).

Dipole Response Function from Spiking Activity

To calculate the current dipole associated with neural spiking activity, a current was injected directly into the soma of the cell via the NEURON IClamp function. For both chattering and regularly spiking pyramidal cell models a current of 0.12nA was injected for 400ms. For the spiny stellate cell model a current of 0.07nA was injected into the soma for a duration of 400ms.

Dipole Response Function from Post Synaptic Potentials

Creating a separate DRF for every synapse location on a neuron becomes computationally infeasible for networks with thousands of neurons and tens of thousands of synapses. To create a more scalable method of simulating synaptic DRFs a generic spatial average was created. For each cell model, a DRF was created for a generic excitatory post synaptic potential (EPSP) and a generic inhibitory post synaptic potential (IPSP). To simulate synaptic input, a difference of exponentials model was used to calculate a conductance change in the membrane due to activation of ligand gated ion channels in the membrane of the post synaptic cell. The time constant for the rising exponential was set to 1 ms, and the time constant for the decaying exponential was set to 6 ms [9]. The maximum resistance for the synapse was set to 6.5$\mu\Omega$ for excitatory synapses and -6.5$\mu\Omega$ for inhibitory synapses.

According to the open field theory, excitatory (depolarizing) activity in the apical dendrites of a pyramidal cell are responsible for creating the current sink [11]. Therefore, the generic DRF for EPSPs on the apical dendrites was created by running a series of simulations where a synapse was placed separately on each dendritic compartment and the resulting DRF was calculated. The DRFs across dendritic compartments were then averaged to create a spatial average DRF representative of synaptic input across locations on the apical dendritic tree. Inhibitory synapses on pyramidal cells in the cortex are spatially localized to the soma and basal dendrites. Therefore, when estimating the DRF for inhibitory activity, synapses were placed separately on each dendritic compartment in the basal dendritic trees. Finally, since spiny stellate cells have no documented synaptic organization, the entire dendritic tree was used to create the spatial average DRF for the EPSP on the spiny stellate cell.

C. Spiking vs synaptic contributions

Comparing the relative contributions of PSPs to spike-related dipoles can be challenging, since the location and weighting of a synapse can greatly influence the magnitude and duration of the dipole created. To this end we conducted a separate series of simulations on the chattering pyramidal cell model designed to characterize the current dipole generated by excitatory post synaptic potentials that result in a somatic membrane voltage just below the threshold potential for an action potential. We conducted 9 simulations with varying numbers of synapses (2-10) located on the most distal portions of apical dendrites. We started with 2 synapses because a single synapse in a distal apical dendrite cannot generate enough current to cause a spike. For more than 10 synapses the entire apical tree was depolarized.

SECTION III. Results

Fig. 1 (top row) shows the spike related DRFs for the cell models examined in sec. II-B. The spike-related DRF for the chattering pyramidal cell shows a spike in the DRF corresponding to each action potential together with a persistent negative envelope in the dipole that persists for the duration of the spiking activity consistent with [8]. The spikes had an amplitude of approximately 0.32 pA-m, while the amplitude of the envelope was -0.41 pA-m. The duration of the dipole activity associated with each spike was approximately 8-10 ms, which is considerably longer than the action potential itself (~1-2 ms). The duration of the envelope was approximately 50 ms (determined as the time from the onset of the first spike to the time the envelope decayed to 5% of its peak value). The spike-related DRF for the regularly spiking pyramidal cell had an initial spike with an amplitude of 0.325 pA-m and duration of 3 ms. The accompanying afterhyperpolarization had an amplitude of -0.1 pA-m and a duration of 18 ms. In contrast, the spike-related DRF for the the spiny stellate cell had an initial spike amplitude of -0.27 pA-m that lasted 0.8 ms followed by an afterhyperpolarization with an amplitude of 0.14 pA-m and duration of 5.6 ms.

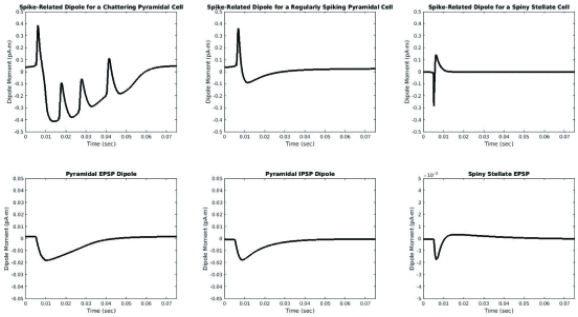

Fig. 1. Dipole Response Functions (DRFs) associated with spiking and synaptic activity. (Top row) DRFs in response to an action potential generated through direct injection of current to the somas of a chattering pyramidal cell (top left), regularly spiking pyramidal cell (top middle), and spiny stellate cell (top right). (Bottom row) Spatial average DRFs in response to sub-threshold synaptic input for an EPSP on a pyramidal cell (bottom

left), IPSP on a pyramidal cell (bottom middle), and an EPSP on a spiny stellate cell (bottom right). Note the change in scale on the y-axis from the top row to the bottom row as well as between PSPs on the pyramidal cells versus the spiny stellate cell.

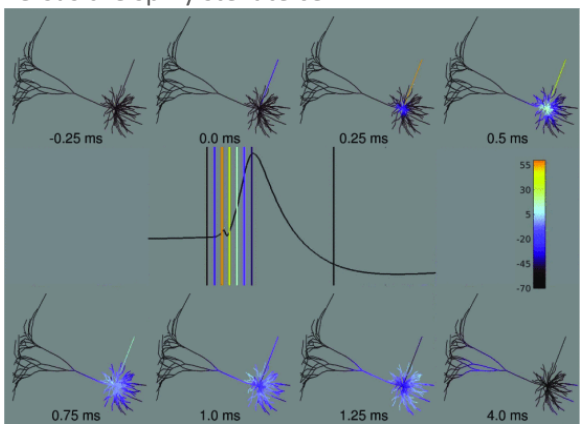

Fig. 2. Time-lapse of membrane voltage for a regularly spiking pyramidal cell during an action potential. The top and bottom rows shows the spatial distribution of membrane voltage across the cell. Changes in membrane potential are coloured relative to the resting potential. The middle plot shows the DRF for the regularly spiking pyramidal cell shown in Fig. 1. The vertical lines indicate where the individual frames of the time-lapse are taken from. The color of each vertical line denotes the membrane voltage change of the axon for easier reference. Time stamps on the bottom of each frame are referenced from the initiation of the action potential.

The DRFs resulting from post-synaptic potentials are shown in Fig. 1 (bottom row). The amplitude of the EPSP on the pyramidal cell was -0.0217 pA-m, while the amplitude of the IPSP on the pyramidal cell was -0.0290 pA-m. The duration of the EPSP was ~36 ms (determined as the time from onset until the PSP decayed to 5% of its peak value), while the duration of the IPSP was ~42 ms. The DRF for the EPSP on a spiny stellate cell was biphasic, with an amplitude -0.0017 pA-m and a duration of 5 ms for the initial negativity. The subsequent positive wave had an amplitude of 0.0003 pA-m and duration of 35 ms.

Examination of the spatial distribution of membrange voltage changes showed that the spike-related DRFs were not generated directly by the action potential, but rather by the backpropagation of currents up the dendritic tree due to an excess of current generated at the axonal hilloc by the action potential. This effect is illustrated in Figs. 2 and 3. Fig. 2 shows the membrane voltages of a regularly spiking pyramidal cell in snapshots across time. The action potential can be seen forming in the axon at the 0 ms snapshot. Within 1 ms the action potential propagated the length of simulated portion of the axon. At the same time excess current propagated from the soma and axonal hilloc into the dendritic tree. The spike-related current dipole reached peak magnitude after approximately 1.25 ms, and lasted 3 ms; 2 ms after the action potential propagated the length of the simulated axon segments.

The impact of backpropagating currents on the DRF was more pronounced for the chattering pyramidal cell (Fig. 3). Following the generation of the initial action potential (seen at the 0 ms snapshot) the current propagated up the dendritic tree. After the backpropagation of current from the initial action potential faded, a persistent depolarization remained in the apical dendrites (see snapshots at 4.5 ms and 11.5 ms), which continued for the duration of the DRF (snapshots 4.5 ms - 52.5 ms)

Fig. 4 shows the traces of the synaptic dipoles created by a varying number of excitatory synapses resulting in a somatic membrane voltage just below the threshold potential. The figure shows a remarkably consistent minimum dipole response with a mean of −0.21±0.02 pA-m, which corresponds to the largest dipole that can be created by EPSPs without generating an action potential (assuming no inhibitory activity). The amplitude is

roughly half that of the envelope of the spike-related dipole for a chattering pyramidal cell (−0.21 ± 0.02 pA-m vs −0.41 pA-m respectively).

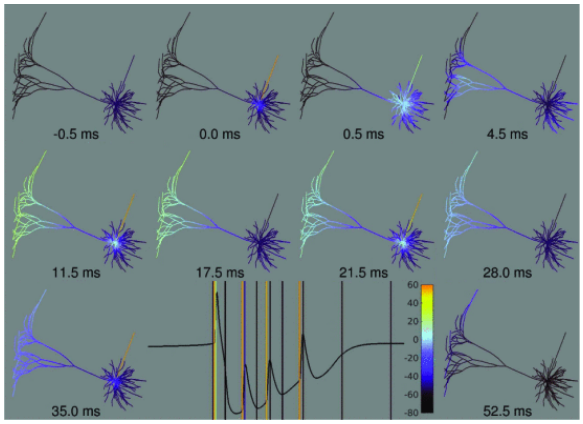

Fig. 3. Time-lapse of membrane voltage for a chattering pyramidal cell during an action potential. Individual plots of the pyramidal cell show the spatial distribution of membrane voltage across the cell. Changes in membrane potential are colored relative to resting potential. The bottom center plot shows the DRF for the chattering pyramidal cell as seen in fig. 1. The vertical lines indicate where the individual frames of the time-lapse are taken from. The color of each vertical line denotes the membrane voltage change of the axon for easier reference. Times are referenced to the initiation of the initial action potential.

SECTION IV. Discussion

Post synaptic potentials are considered to be the leading contributor to EEG signals because they last considerably longer than action potentials [10], 10-30 ms vs 1-2 ms respectively. However, our simulations indicate that the current dipoles generated by spiking neurons are not driven by the action potential, but by the backpropagation of current from the axonal hillock into the dendrites. This backpropagation effect leads to current dipoles which can last considerably longer than the 1-2 ms time-frame typically associated with spiking activity. The spike-related dipole of an individual action potential for a chattering pyramidal cell lasted close to 8 ms while the envelope lasted over 50 ms. The duration of the envelope was longer than that of the typical post synaptic potential providing additional time for the summation of spike-related dipole activity. Interestingly, even for regularly spiking pyramidal cells, afterhyperpolarization in spike-related current dipoles lasted for up to 18 ms. This is roughly half the duration of an EPSP on the pyramidal cell (36 ms), but considerably longer than the 1-2 ms duration usually associated with spiking activity.

In the final set of simulations we took the first steps toward characterizing the relative dipole contributions of EPSPs versus spike-related dipoles. These simulations show that the current dipole moment associated with excitatory synapses necessary to generate an action potential was approximately half the size of the envelope created in the spike-related current dipole of a chattering pyramidal cell. Additionally, the DRF for a regularly spiking pyramidal cell had an amplitude which was half that of the dipole generated by apical EPSPs. This suggests that spiking activity could contribute in a meaningful way to the current dipoles associated with EEG. Future work will to incorporate the DRF structure into networks of neurons in which the balance of excitatory and inhibitory connections can be established in an active network. In order to better understand the neural computations underlying EEG it is important to understand how individual neurons contribute to dipole layers on the cortical surface. This research takes the first steps toward that goal.

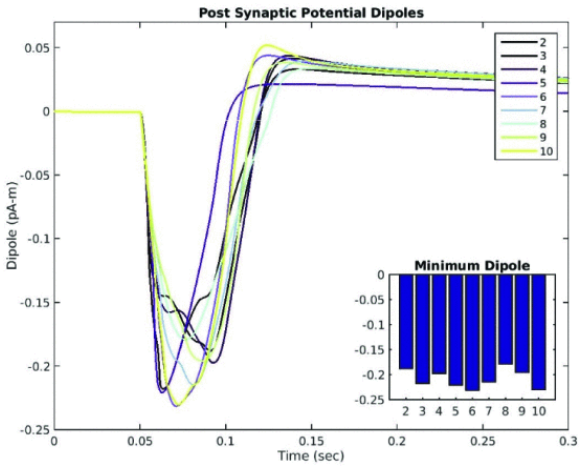

Fig. 4. Traces of the EPSP synaptic current dipole generated by excititory synapses on the apical dendrites of a pyramidal cell. The number of synapses in each simulations varied from 2 to 10. For each simulation the strength of the synapses was scaled to provide the maximal sub-threshold membrane depolarization at the soma. Bar graph shows peak dipole value for each simulation.

References

1.R. Lorente de No, "A study of nerve physiology", *Rockefeller Institute*, vol. 132, 1947.

2.M. X. Cohen, "Where does eeg come from and what does it mean?", *Trends in Neurosciences*, vol. 40, no. 4, pp. 208-218, [online] Available: http://www.sciencedirect.com/science/article/pii/S0166223617300243.

3.N. T. Carnevale and M. L. Hines, The NEURON Book, Cambridge University Press, 2006.

4.R. A. McDougal, T. M. Morse, T. Carnevale, L. Marenco, R. Wang, M. Migliore, et al., "Twenty years of modeldb and beyond: building essential modeling tools for the future of neuroscience", *Journal of Computational Neuroscience*, vol. 42, no. 1, pp. 1-10, Feb 2017, [online] Available: https://doi.org/10.1007/s10827-016-0623-7.

5.Z. F. Mainen and T. J. Sejnowski, "Influence of dendritic structure on firing pattern in model neocortical neurons", *Nature*, vol. 382, pp. 363-366, July 1996.

6.A. C. Guyton and J. E. Hall, Textbook of Medical Physiology, W.B. Saunders Company, 1996.

7.J. Riera, T. Ogawa, T. Goto, A. Sumiyoshi, H. Nonaka, A. Evans, et al., "Pitfalls in the dipolar model for the neocortical eeg sources", *Journal of Neurophysiology*, vol. 180, no. 4, pp. 956-975, 2012.

8.S. Murakami and Y. Okada, "Contributions of principal neocortical neurons to magnetoencephalography and electroencephalography signals", *The Journal of Physiology*, vol. 575, no. 3, pp. 925-936, 2006.

9.W. Gerstner, W. Kistler, R. Naud and L. Paninski, *Neuronal Dynamics online book: From single neurons to networks and models of cognition*, 2014, [online] Available: http://neuronaldynamics.epfl.ch/online/Ch3.S1.html.

10.F. Lopes da Silva, EEG - fMRI: Physiological Basis Technique and Applications, Heidelberg:Springer-Verlag Berlin, pp. 19-38, 2010.

11.P. Olejniczak, "Neurophysiologic basis of eeg", *Journal of Clinical Neurophysiology*, vol. 23, no. 3, pp. 186-189, June 2006.